From the Conformation of a Single Molecule to Physical Networks in Highly Interacting Polymers: A Small-Angle Neutron Study

DVORA PERAHIA, XUESONG JIAO,* RAKCHART TRAIPHOL†

Department of Chemistry, Clemson University, Clemson, South Carolina 29634-0973

Received 11 November 2003; revised 14 April 2004; accepted 28 April 2004
DOI: 10.1002/polb.20182
Published online in Wiley InterScience (www.interscience.wiley.com).

ABSTRACT: Small-angle neutron scattering has been used to study the conformation and structure of highly interacting macromolecules in complex fluids. The evolution of the structure has been investigated from the conformation of a single molecule through an association process to the formation of physical networks. Two highly interacting polymers, an ionic polymer (consisting of a perfluorinated backbone and an ionizable hydrophilic side chain dissolved in water/alcohol mixtures) and rodlike, highly conjugated phenylene ethylene molecules (dissolved in toluene), have been studied. Highly interacting polymers often form relatively long lasting physical networks with increasing polymer concentration. The driving force, however, is system-specific, and so are the micellar systems and physical networks formed. Although the two families of polymers under consideration are entirely different chemically, their strong interaction, either ionic or through π–π coupling, results in similarities in the complex fluids formed when they are dissolved in solutions. These include elongated configurations in dilute solutions, association into micelles, and eventually coalescence into physical networks. The ionic polymers form durable stable networks, whereas the rodlike polymers form a fragile, gel-like phase. © 2004 Wiley Periodicals, Inc. J Polym Sci Part B: Polym Phys 42: 3165–3178, 2004

Keywords: micelles; physical networks; perfluorosulfonimide ionomers; polymer electrolytes; small-angle neutron scattering; gels; colloids

INTRODUCTION

This article reports the contributions of small-angle neutron scattering (SANS) to the understanding of the molecular configuration and association modes of highly interacting polydispersed polymers in solutions. A unique aspect of highly interacting polymers is that these macromolecules associate into distinct structures and exhibit well-defined electronic or ionic transport characteristics despite the diversity in their chemical structure. The variability in the chemical structure includes polydispersity and a noneven distribution of highly interacting groups along the backbones of the polymers. Understanding their structure and dynamics becomes an important challenge for the discernment of the basic physics that govern highly interacting polymers and as a result leads to new applications. This study focuses on two groups of highly polydispersed macromolecules, including ionic and highly conjugated polymers.

Ionic polymers, often called ionomers or ion-containing polymers, consist of hydrophobic, hy-

*Present address: APS, Argonne National Laboratory, 9700 South Cass Avenue, Argonne, Illinois 60439
†Present address: Chemistry Department, Naresuan University, Phitsanulok 65000, Thailand
Correspondence to: D. Perahia (E-mail: dperahi@ces.clemson.edu)

Journal of Polymer Science: Part B: Polymer Physics, Vol. 42, 3165–3178 (2004)

drophilic, and ionic groups. Their technological uses include many electrochemical applications, such as batteries and fuel cells. They are also used as proton-exchange membranes for separation as well as drug-delivery systems.[1–5] The second class of highly interacting polymers addressed in this work includes conducting and semiconducting polymers. These consist of either conjugate backbones or chemical groups that can facilitate charge transfer. Many of their future applications will involve the miniaturization of electronic and electrooptic devices.[6–10]

Highly interacting polydispersed polymers are of particular interest because different energy scales simultaneously control the conformation and association of the macromolecules. Van der Waals interactions, affecting short-range, angstrom-to-nanometer length scales, coexist with stronger forces, such as ionic or aromatic couplings, that affect up to 100-nm periodicities in the same complex fluid.

Studying the structures of these complex fluids requires probing dimensions from several angstroms to the nanometer length scale, at which individual polymer molecules can be detected, to the 100-nm range, at which the aggregates and correlations within networks can be observed. The technique must also be sensitive to small changes in amorphous media. With the natural difference in the scattering length densities of hydrogen and deuterium and in the scattering length densities of hydrogen and fluorine, SANS has been at the core of the investigation of structure and association in polymeric systems.[8–12] These studies span a wide range of phenomena. Recent studies include polymers in supercritical fluids,[13] complex fluids such as starlike dendrimers in solution, microemulsions, micelles, diblock copolymers,[14–17] ionic polymers,[18–21] blends,[22–24] and the association of macromolecules in biological systems.[25] The association of monodispersed, nonionic, flexible diblock and triblock copolymers as well as ionic polymers with well-defined molecular weight distributions and ionic strengths has been the subject of many studies.[18–29]

The driving force for the association of the polymers is rather universal. Entropy favors mixing while reducing the interactions between incompatible components (or increasing the interactions between compatible ones), and this results in segregation into a variety of structures, from highly organized phases to physical networks to random clusters.[1–2,29] The forces and the association phenomena are universal, but the nature of the structures formed is system-specific.

Obtaining a basic understanding of the conformation and association of polydispersed, highly interacting polymers on the level that exists for small surfactant molecules and diblock copolymers will allow the development of theoretical insights into these important complex fluids.

In this study, perfluorosulfonimide and dialkyl poly(*p*-phenylene ethynylene) (PPE) rigid and aromatic macromolecules in solutions have been examined over a wide concentration range with SANS. These polymers have been chosen because of our ability to modify their chemical structure in a controlled way;[30–32] this allows a correlation between the molecular architecture and the structure of the complex fluid. Although the chemical structure can be modified, the systems remain polydisperse with a high degree of variability in both the molecular weights and equivalent weights (EWs).

The basic concepts of SANS relevant to the current study are briefly reviewed and are followed by the experimental details. The results for the two different systems are given and are followed by a summary of our findings.

SCATTERING OF POLYMERS IN SOLUTIONS

In amorphous media, the interference of the incident wave with the heterogeneities in the material provides structural information. These heterogeneities may be several to hundreds of radiation wavelengths long.[29] In amorphous polymers and polymer solutions, structural information such as the concentration fluctuation, shape and size, number of objects, and long-range correlations is expressed in the scattering patterns at small angles. The scattering of polymers shows different dimensions, depending on the q range of the measurement and its relation to the dimension of the polymer. q is the momentum transfer, which is defined as $q = 4\pi/\lambda \sin(\theta/2)$ (θ is the scattering angle with respect to the incident beam path).[29,33–34] Figure 1 presents a schematic representation of different length scales in a solvated polymer as a function of the relation between q, the persistence length (l_p), and the radius of gyration (R_g) of the polymer. The exact dimensions depend on the molecular weight of the polymer and its interactions with the environment. If the polymers are fully solvated, at small q [Fig. 1(I)], at which qR_g approaches 0, each polymer molecule forms a random coil that is viewed as a center of mass. With increasing q [Fig. 1(II)], at which

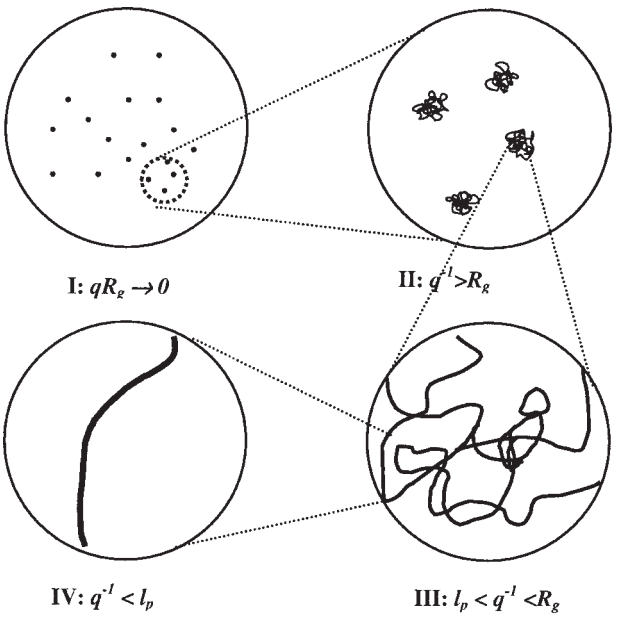

Figure 1. Schematic representation of the part of the polymer viewed at different length scales with respect to l_p and R_g.

q^{-1} is greater than R_g, the entire dimension of the coil is depicted, and R_g is measured. In this domain, the size of the coil is well described by a Guinier approximation.[25–26] Further increasing q to $l_p < q^{-1} < R_g$ results in an insight into the segmental distribution within the coil [Fig. 1(III)]. Finally, for $q^{-1} \ll l_p$, the chain appears completely rigid [Fig. 1(IV)]. Tuning the q range of the measurement allows us to focus on different length scales.

The relation between the smallest rigid segment of the polymer and its total dimension determines many of the properties of polymers, and as such, numerous studies have been focused on the determination of l_p of the polymer. The polymers addressed in this work exhibit large l_p's because of the presence of ionic groups and highly conjugated backbones. For nonionic polymers, l_p is a direct function of the inherent rigidity of the monomer. In ionic systems, in addition to the effects of the chemistry of the backbone, the charge often dominates the conformation of a single molecule in any environment in which the ions can dissociate.[35] Unscreened electrostatic interactions due to the ionization along the backbone of the polymer will tend to increase the local rigidity and the global size of the polyion. With a mean-field approach for polyelectrolytes, the total l_p is divided into an intrinsic component (l_0) and an electrostatic component (l_{el}). The last depends on electrostatic screening in different environments, including the ionic strength due to counterions and the external salt concentration. When l_{el} is less than l_0, the Odijk–Skolnick–Fixman model, which correlates a structural charge parameter (ξ), the Bjerrum length (l_B), and the Debye Hückel screening parameter (k), such that l_{el} is equal to $\xi^2/4k^2l_B$ and l_B is equal to $e^2/\epsilon_0 K_B T$ (where e is the electron charge, ϵ_0 is the electrical permittivity of the solvent, T is the temperature, and K_B is Boltzmann's constant), has been used to extract l_p of polyelectrolytes.[35]

In general, the scattering intensity as a function of q is given by[25–27,29,33–35]

$$I(q) = AI_0NV^2(\Delta b_v)^2P(q)S(q) + B_{inc}$$

where I_0 is the intensity of the incident beam and A is a constant that encapsulates instrumental factors. N is the number concentration of scattering objects, V is the volume of one scattering particle, $(\Delta b_v)^2$ is the scattering contrast term, and $P(q)$ is the form factor. It describes the scattering interference of a single particle. $S(q)$ is the structure factor, describing the interference between scattering from different objects, and B_{inc} is the incoherent scattering. This study focuses on dilute solutions in which the scattering profile is dominated by $P(q)$. The form factors relevant to this study and the corresponding approximations are presented in the analysis of each of the systems. For a polymer with well-defined molecular weights and EWs (a measure of the size of the mass of the polymer between two consecutive ionic groups along an ionic polymer backbone), $P(q)$ can be obtained analytically for all of the aforementioned ranges. When the polymers are highly polydispersed or the location of the ionic groups along the polymer diverges from a random distribution, scaling arguments become essential for analyzing the results.

Experimental

Scattering

SANS experiments were performed on the NG3 30M SANS instrument at the Center for Neutron Research at the National Institute of Standards and Technology and on SAD (small angle diffractometer) at the Intense Pulse Neutron Source of Argonne National Laboratory.

NG3 30M SANS. Three sample-to-detector distances of 2, 5, and 13.10 m were chosen with a

neutron wavelength of $\lambda = 6$ Å and a $\Delta\lambda/\lambda$ value of approximately 10%; this resulted in a q range of $0.004\ \text{Å}^{-1} < q < 0.4\ \text{Å}^{-1}$. The measurements were carried out at 20 ± 0.5 °C.

SAD. SAD is a time-of-flight small-angle diffractometer with a sample-to-area-detector distance of 1.504 m. The pulse consists of neutrons with a wavelength span of 0.9–14 Å, encapsulating a q range of 0.005–0.35 Å^{-1}. The acquired scattering intensity was converted into an absolute intensity scale by normalization to the flux of the direct beam.

Protonated and deuterated solvents were used, depending on the polymer. For perfluorinated materials, the large contrast in the coherent scattering length (b) between protons ($b = -0.3741 \times 10^{-12}$ cm) and fluorine ($b = +0.565 \times 10^{-12}$ cm) permitted the use of protonated solvents. For protonated polymers, deuterium-labeled ($b = +0.6671 \times 10^{-12}$ cm) solvents were used.

The samples were encapsulated in 1-cm-diameter cells, consisting of quartz windows separated by 2-mm spacers. The temperature was controlled with a water bath (±0.5 °C). One-dimensional scattering patterns, normalized to the scattering of a standard and to the scattering from the solvents, from which the solvent signal, measured at each individual temperature, was subtracted, were obtained via radial averaging over the detector area.

Data Fitting. For each of the systems, numerous plausible models were fit to the experimental data. For PPE, for which no prior knowledge was available, the models were chosen in accordance with supporting atomic force microscopy data of trapped molecules from the complex fluid at different concentrations and with calorimetric data, which assisted in the estimation of the number of π–π bonds in the system. For the ionic polymers, a vast amount of knowledge exists and has been applied. For this study, an acceptable fit is defined as matching the experimental data with a divergence of less than 1%. Therefore, all fits presented are within this error range. All original data sets are presented with error bars. When plotting variation plots (e.g., Guinier and Kratley plots), we chose to omit some of the error bars to demonstrate the quality of the fitting.

Polymers

Perfluorosulfonimide ionomer in its acidic form, with a weight-average molecular weight of approximately 1×10^6 g mol^{-1}, a weight-average molecular weight/number-average molecular weight (M_w/M_n) ratio of approximately 6, and an EW of 1200, was synthesized via emulsion polymerization. The EW is a measure of the ionic density along the chain and is expressed as the weight of the repeat unit between two adjacent ionic groups. EW was determined by the titration of the ionomer with NaOH. The average number of repeating units between ionic group n was calculated to be approximately 5.5. The distribution of the ionic groups along the backbone was assumed to be random, but some blocks may exist. Solutions were made through the dissolution of the polymer at 250 °C under pressure; colorless, homogeneous, and transparent solutions were formed.[36,37]

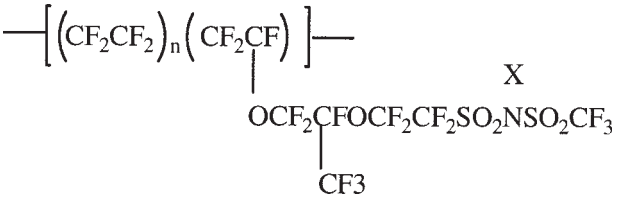

Figure 2. Chemical structures of perfluorinated ionomers (PFSI). *X* can be any counterion. In this study, *X* is a proton.

Dinonyl PPE molecules with a polymerization number of 82 and an M_w/M_n value of 2 were dissolved in toluene-d_8 (Cambridge Isotope Laboratories). The polymerization number was determined by gel permeation chromatography with a saturated analogue of the conjugated molecule.[31–32]

ASSOCIATING IONIC POLYMERS

Introduction

The molecular conformation and the association of the perfluorosulfonimide ionomer, the chemical structure of which is shown in Figure 2, in water/alcohol solutions have been studied as functions of the concentration at different temperatures. The solvent was chosen because of the relatively high solubility of the ionomer in that mixture and the technological need to understand the behavior of these types of polymers in the presence of water and alcohol.[4]

Several studies have followed the evolution of the structure of ionic polymers as the melts of different ionomers swell with polar solvents.[38–42] These studies have shown that with increasing

solvent content, ionic domains grow into bicontinuous channels. A further increase in the solvent content results in dissociation into large domains and eventually micelles. The driving force for the different structures, minimizing the interaction between noncompatible parts, is well established. There are, however, several open questions that are at the core of understanding the structure and dynamics of these complex polymers. These include the structure of highly rigid ionic polymers, the dissociation of the network into well-defined micelles, and the coalescence of the micelles into well-defined networks, despite the large variability in the chemical structure and the association process of single molecules into relatively monodispersed micelles.

The conformation of perfluorinated ionomers in water or alcohol is a result of three factors: the interaction of the Teflon-like backbone, which would collapse in a polar solvent; the solvation of the side chains; and the stabilization of the ionic groups, which tend to expand the molecule. The configuration of an isolated macromolecule is expected to affect the association into micelles. The overall size of the polymer, as represented by R_g, allows us to estimate the overall configuration of the polymer. A soluble polymer, with $l_p \ll R_g$, assumes characteristic dimensions reflecting its polymerization number (N), its l_p value, and its interactions with the solvent. R_g of the polymer scales as a power law with the polymerization number: $R_g \sim N^{\nu}$. For a good solvent, ν is 3/5, and the chain is expanded. For a poor solvent, ν is 1/3, and the chain collapses. In an ideal solution (θ solvent), ν is 1/2, at which a Gaussian chain is expected.[28,29,34,43]

Results and Discussion

SANS measurements were carried out on solutions of the ionomer in 1:1 water/ethanol solutions. Figure 3(a) presents the changes in the neutron scattering intensity [$I(q)$] as a function of q as the concentration of the polymer is varied from 0.2 to 1.6 wt % at 25 °C. Increasing the concentration above approximately 2 wt % results in phase separation unless salt is added. With increasing concentration, the signal-to-noise ratio increases. The increase is accompanied by a clear change in the dependence of the scattering intensity as a function of q. We often refer to this change as a change in the line shape.

In comparison with surfactant systems, at low enough concentrations, below a critical micelle concentration, the solution consists of isolated molecules. The ionomer in this study is dissolved in a polar solvent. Thus, it is expected to assume a conformation that would minimize the interac-

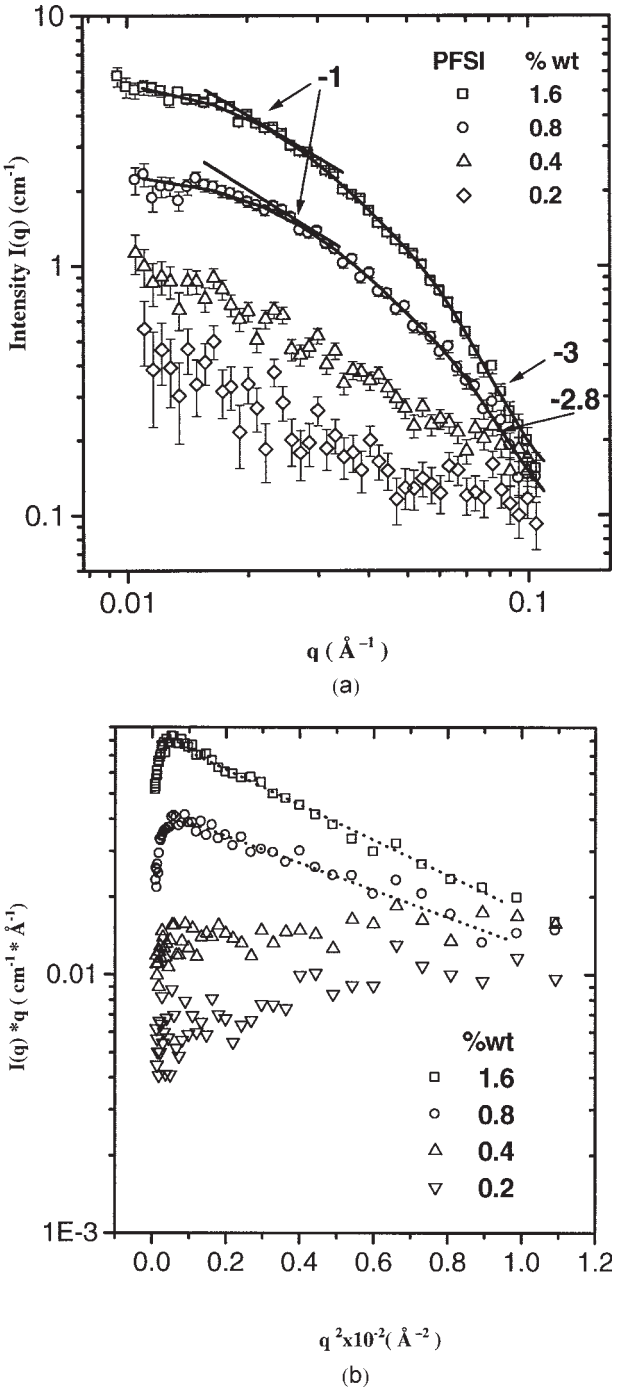

Figure 3. (a) SANS patterns of different samples of the ionomer in a 1:1 water/ethanol solvent at the indicated concentrations (the symbols correspond to the experimental data, and the solid lines correspond to the fits to a cylindrical form factor) and (b) Guinier plots of the data (the divergence of the fits is less than 0.5%).

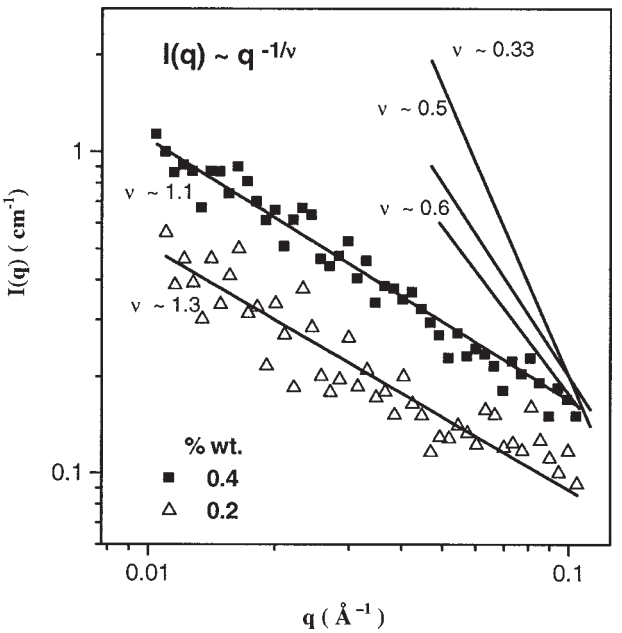

Figure 4. Scattering patterns (0.4 and 0.2 wt %) in an intermediate q range plotted as a function of q, providing linear dependence with the indicated ν indices (the divergence in the fit is less than 0.5%).

tion of the Teflon-like backbone with the solvent. Plotting $I(q)$ at an intermediate range (Fig. 4; $1/l_p < q < 1/R_g$) as a function of q yields slopes of 0.9 and 0.8 for the two lower concentrations, 0.2 and 0.4 wt %. For polymer chains, $I(q)$ is approximately equal to $q^{-1/\nu}$, and this results in ν values of 1.1 and 1.3 for the corresponding slopes. Both values are larger than 0.6, the value expected for a flexible chain in good solvents.

These exponents indicate that the polymer chains are extended beyond the dimensions expected for a random coil in a good solvent. This has been observed in different polyelectrolytes, in which the electrostatic interactions become significant.[35] As discussed previously, the scattering pattern of a polymer chain depends on both the dimensions of the polymer molecules and the length scale measured. As long as the chain is long enough and the q values are sufficiently low ($R_g q \ll 1$), the scattering intensity can be described by the Debye form factor. As we zoom into smaller length scales, the chain structure is dominated by l_p, resembling rods rather than coils.[29,33,34] For wormlike chains, the crossover region can be described by the Sharp–Bloomfield function, which consists of weighted Debye and rodlike components.[34,44]

The polydispersity of the ionomer prevents a quantitative analysis of the rod–coil crossover. Therefore, the data have been evaluated qualitatively instead of being directly fit to the Sharp–Bloomfield function. A plot of $q^2 \ln(q)$ versus ql_p (Kratky plot), is shown in Figure 5(a), which illustrates the crossover from a random coil of the chain to an extended thin rod. At low q values, the scattering profile provides information on the overall dimensions of the polymer. Beyond a certain q value, defined as the crossover, the scattering is dominated by l_p. Figure 5(b) shows a Kratky plot of the patterns obtained for the two low-concentration solutions; the rodlike region can be clearly observed, but the crossover region is not apparent. This is consistent with a rigid chain: over the measured q range, only l_p of the extended

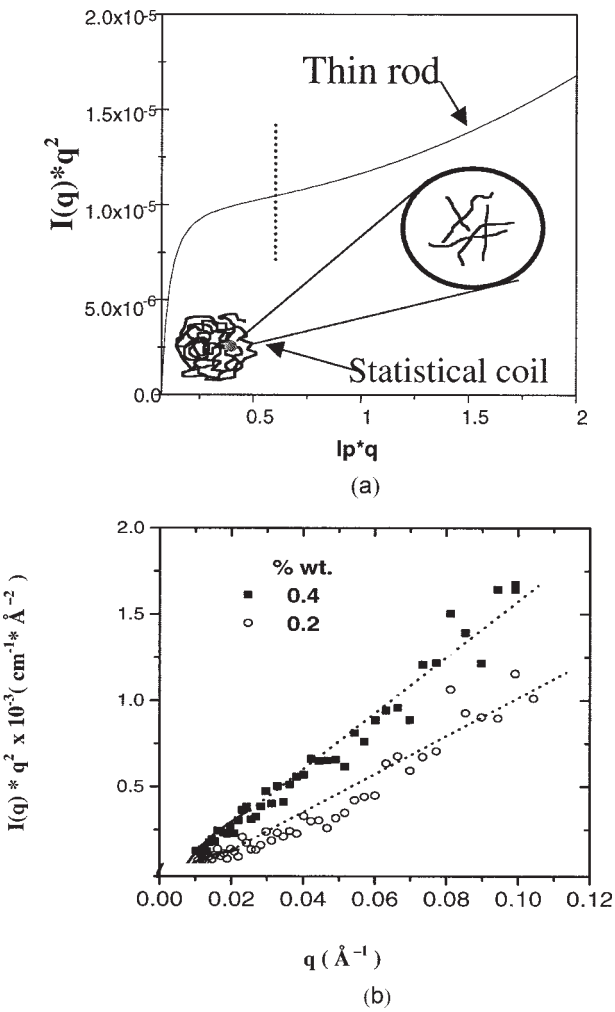

Figure 5. (a) Theoretical Kratky plot showing the random coils becoming rodlike beyond the crossover (marked by a dashed line) at a short distance and (b) Kratky plots of $I(q)q^2$ versus q at two low concentrations (0.4 and 0.2 wt %) indicating the rigid-rod structures of the isolated molecules.

chain contributes to the scattering. The slopes in Figure 4 are close to −1, which is characteristic of the scattering of a rigid rod, indicating that the isolated ionomer molecules behave like infinite rods within the studied q range. This result is rather surprising because the samples do not contain any additional salt and are charge-balanced. Moreover, the Teflon-like backbone is in a poor solvent, and the density of the polar side chains that solvate the molecule is relatively low. Therefore, the chain is expected to assume a collapsed configuration. This apparent stiffness of the isolated chains is consistent with highly charged polyelectrolytes with low EWs (dense ionic groups). This, however, is not in agreement with the EW and the ionic strength of the solution. Therefore, we assume that the distribution of the ionic groups along the backbone is not random and that small ionic blocks are formed.

As for surfactant systems, one would expect that with increasing concentration, isolated molecules would associate into micelles.[38] A first indication of the formation of micelles can be obtained from the slope of the SANS profiles at an intermediate q range, above 0.6 wt %. At high concentrations (0.8 or 1.6 wt %) and low q values, a power-law dependence of q^{-1} can be observed, as shown by the tangential lines in Figure 3(a), which are typical of elongated objects. At high q, slopes of about −3, characteristic of the scattering of a cross section of cylinders, are measured. The profiles of these two concentrations have been fitted to a form factor of a cylinder. This is consistent with previous findings of cylindrical micelles in Nafion solutions, a commercially available perfluorinated ionomer. These cylindrical micelles in polar solvents consist of a Teflon-like core and ionic/polar side chains at the periphery, surrounded by solvent molecules. Although the molecular weight of the polymer is rather high, the pattern does not consist of an interaction peak within the studied concentration range. The data have thus been modeled with a form factor of noninteracting cylindrical objects.

For noninteracting cylindrical objects, $I(q)$ can be described by $I(q) = L(\pi/q)I_c(q)$. $I_c(q)$ is given by $I_c(q) = (\Delta\rho)^2 A \int 2\pi r dr \gamma_{co}(r) J_0(qr)$, where $\Delta\rho$ is the scattering contrast, A is the cross-section area, $\gamma_{co}(r)$ is the correlation function of the cross-section geometry, J_0 is the zero-order Bessel function, and L is the length of the cylinder. For the intermediate part of q, the intensity of the cross section dominates the scattering. Therefore, the intensity can be expanded into a power series of R_c, the radius of gyration of the cross section ($R_c = R/\sqrt{2}$) where R is the radius of the cylinder, and $I(q)$ can be approximated by $I(q) = (I_0/q) \exp(-q^2R_c^2/2)$. Accordingly, for a cylindrical object, a Guinier plot of $\ln[qI(q)]$ as a function of q^2 results in a linear relationship, as presented in Figure 3(b) for the same data presented in Figure 3(a). The curves of 1.6 and 0.8 wt % solutions form a straight line in the intermediate q region. Both Guinier plots and the fits to a cylindrical form factor yield very good agreement with the experimental data. These correspond to cylinders with an R value of 27 ± 3 Å and a length of 160 ± 15 Å for the 0.8 wt % solution and with an R value of 31 ± 4 Å and a length of 185 ± 20 Å for the 1.6 wt % solution. The fits yield less than 0.5% error. The error is, therefore, estimated from multiple measurements. Both the radii and lengths of the cylinders increase slightly with increasing concentration. The analysis of the length is limited by the lowest q range that could be measured by SANS.

The micelles appear to be surprisingly well defined for a polymer with such a broad distribution of molecular weights and a large diversity in the distribution of ionic groups along the backbone. It suggests that a balance between the cohesive energy, surface tension, and columbic interactions takes precedence over the effects of the molecular weights.

An interesting concentration regime is that in which the micelles coalesce into a thin film. According to the phase diagram proposed by SANS and small-angle X-ray studies for other perfluoroionomers, the bulk structure of molecules should consist of spherical or elongated hydrophilic or ionic domains. As we increase the concentration, phase segregation to the swollen polymer and solvent takes place. Allowing the polymer solution to dry results in the formation of a bundle of micelles shown in the STM image[41] in Figure 6. Moreover, these bundles do not coalesce upon the annealing of the sample above the glass transition for the hydrophobic metric (below that of the bulk reported value for the ionic groups). These results suggest that the micelles formed by these ionomers are extremely stable in comparison with both surfactant and micellar phases formed by nonionic polymers.

Conclusions

SANS studies have shown that in dilute polar solvents, the chain configuration of PFSI is dom-

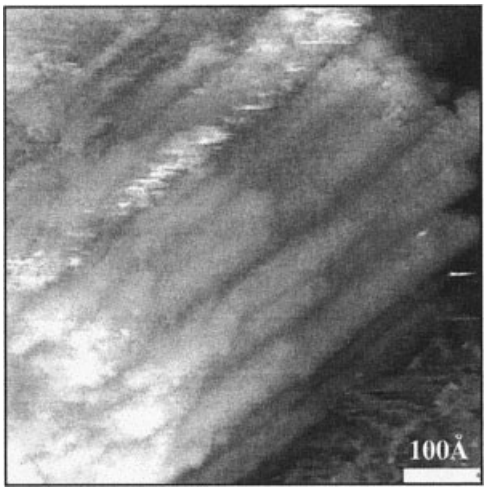

Figure 6. Bundles of cylinder micelles revealed by STM.[41]

inated by the presence of the ionic groups and is expanded, despite the very low solvent quality for the polymer backbone. The results show that the ionomer associates to form extremely stable and relatively monodispersed cylindrical micelles at relatively low concentrations. At very low concentrations (0.4 and 0.2 wt %), the interaction between the charged groups and the polar solvents overcomes the hydrophobicity of backbone, making the ionomer wormlike. With increasing concentration, the electrostatic interactions are not sufficient to maintain the expanded chain configuration, and this results in an association of the hydrophobes to minimize the interaction with the solvent.

A schematic representation of the ionomer in different association modes is shown in Figure 7. In the dilute regime, the dominant species in solution are expanded noninteracting chains. With increasing concentration, the ionomers associate. The clustered structure of the Teflon backbone minimizes the interfacial energies between the hydrophobic groups and the solvents, compensating the reduced entropy due to the constrained configurations in aggregation. Overall, the aggregated polymers have lower chemical potential than the nonaggregated polymers. The dimensions of the aggregates clearly show that the micelles consist of more than one polymer molecule.

ASSOCIATION OF RIGID POLYMERS

Introduction

This part of the study focuses on highly interacting conjugated polymers. It has been established that π–π interactions serve as a driving force for association in many systems, including simple aromatic liquids, discotic liquid crystals, and some polymers.[9] This interaction is definitely smaller than that of ionic associations and is approximately a third of the interaction of an average hydrogen bond. When multiplied, however, by the number of monomers in a polymer, this becomes a significant driving force.

We have recently shown that highly conjugated linear polymers follow the same association trend as ionomers from a single molecule to an aggregate to a physical network as their concentration in a solution of an aromatic solvent increases. In contrast to the physical networks formed by ionomers, these networks are not stable. They break upon a small perturbation.[45–47] This is a characteristic behavior of a fragile phase.[48–53] A wide range of soft materials, such as colloids, emul-

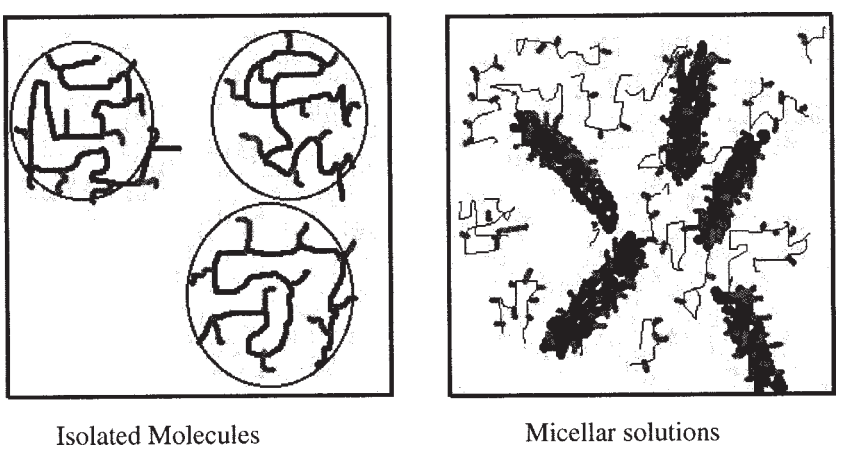

Figure 7. Schematic representation of the aggregation process.

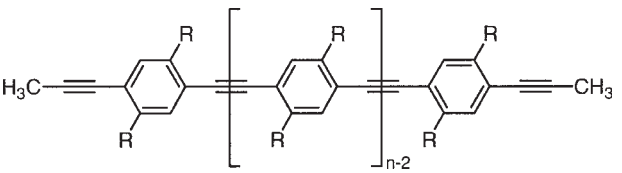

Figure 8. Chemical formula of PPE. *R* represents an alkyl chain, and *n* is the degree of polymerization. In this study, *n* is 9.

sions, and foams, undergo the constraint of their motion at low temperatures or high volume fractions. The constrained gel phase, or jammed phase, is characterized by a solidlike rheological response, and the local dynamics are often rather fast in comparison with that of molecules in a solid.[48–55] In contrast to solids, in this type of fragile matter, changing the direction of the applied stress releases the constraint. These characteristics are typical of numerous systems, from macroscopic granular systems to microscopic molecular clusters. In colloidal systems (rigid particles with no electrostatic interaction), the balance between the thermal energy of a system at a given temperature, $\sim kT$ (where k is the Boltzmann constant and T is the temperature), and the attractive interaction between particles determines the state of the system, that is, fluid or constrained. The same phenomena have been observed in solutions of some polymeric micelles and star polymers, for which cooling or heating leads to the formation of gel-like phases.[54]

Similarly to colloidal systems, the energy balance between particles in complex fluids consisting of clusters of molecules and solvents controls the state of the system. However, changing the temperature in a complex system, which consists of aggregates, is not merely changing just the interparticle interactions and kT. Temperature changes over relatively small intervals may be accompanied by significant changes in the microstructure of the system, and so the formation of a constrained phase is a combination of multiple factors.

Using rodlike oligomers of dinonyl PPEs, in toluene we have studied the structural evolution from a single molecule to constrained phases in complex fluids.[43–45] The molecular structure of PPE is shown in Figure 8. Dilute solutions of PPE in toluene are transparent fluids above room temperature. When they are cooled, a glasslike and yellow phase, which does not flow, is formed and is here called a gel-like phase. The yellow color is an indication of the constraint of the freedom of

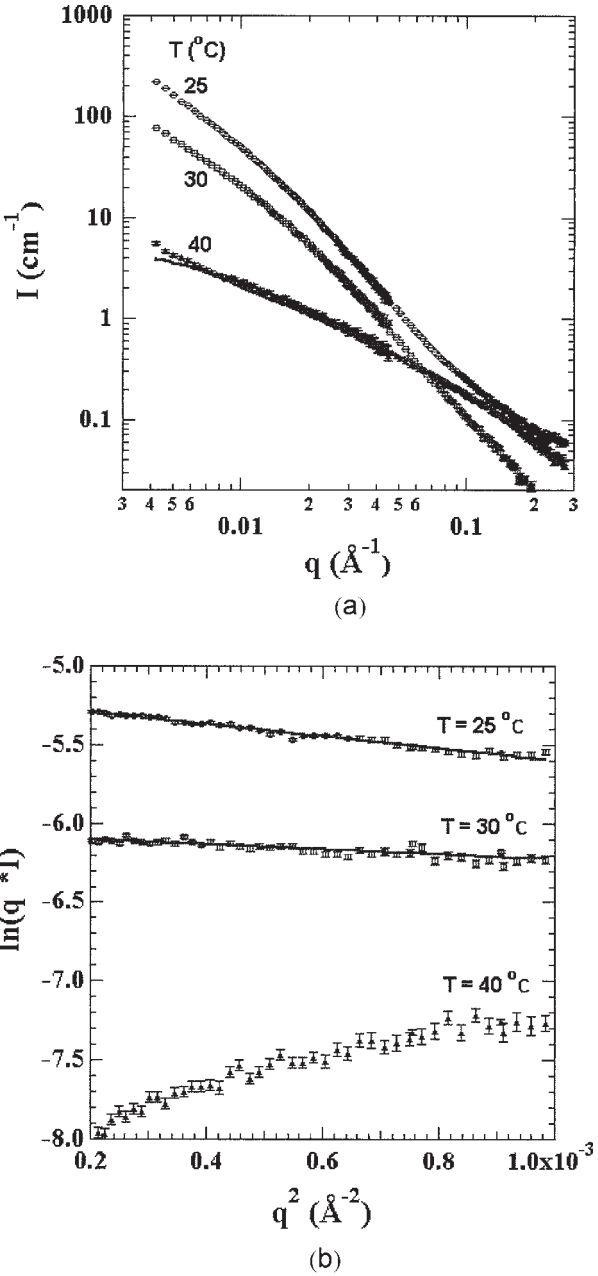

Figure 9. (a) $I(q)$, normalized to the scattering of the solvent, as a function of q at a concentration of 2.13 wt % at the indicated temperatures. The patterns were obtained through the combination of the scattering from two configurations (the detector was placed 3 or 13 m from the samples). The symbols correspond to the experimental data, and the solid lines represent different fittings. The lines fit with less than 1% error. (b) Plot of the low q range of the same patterns, showing linear lines obtained at 30 and 25 °C that are characteristic of large, flat objects. Cylindrical characteristics can be observed at 40 °C. The lines fit with less than 0.5% error.

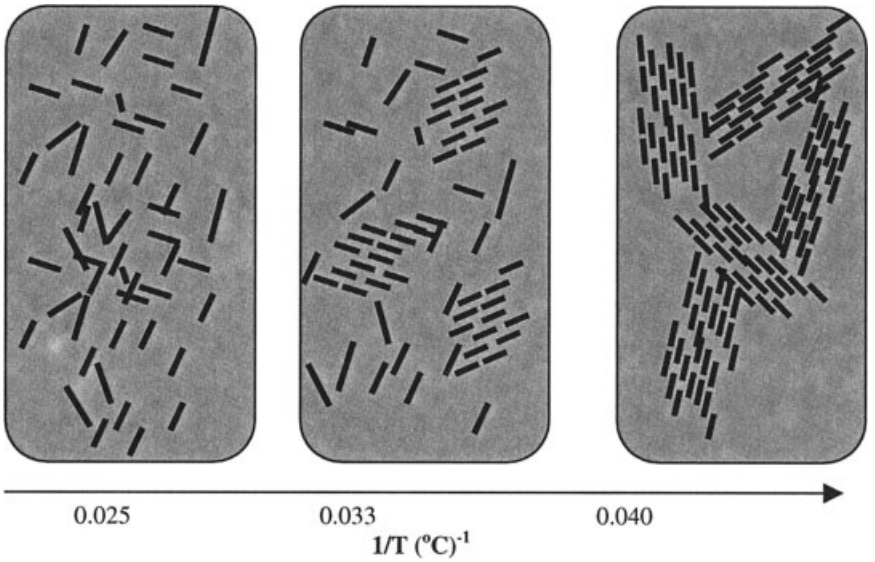

Figure 10. Schematic representation of the association process.

motion of the PPE backbone, which is attributed to the association of the molecules. In contrast to most physical gels, a gentle shear is sufficient to break the gel-like phase and form a liquid. This transition is accompanied by changes in the enthalpy. NMR studies have clearly indicated that this transition is also associated with the constraint of motion of both the PPE molecule and the toluene.[46,47]

Results and Discussion

Patterns for the three different regimes, the isotropic liquid (40 °C), the transition regime (30 °C), and the gel-like phase (25 °C), are shown in Figure 9(a,b) for 2.13 wt % solutions of PPE in toluene-d_8 at different temperatures. At 40 °C, the solutions are optically transparent and fluid. At this temperature, the scattering profile is consistent with the cylindrical form factor given before. Cylinders with characteristic dimensions of $L \sim 641 \pm 15$ Å and a radius of approximately 11 ± 3 Å are obtained. These dimensions are consistent with the size of a stretched PPE molecule of approximately 80 repeating units. The error is determined via averaging over the numbers obtained from the best fit and the largest q range that can be reasonably fit.

A fully extended chain configuration is rather surprising because in the absence of strong electrostatic interactions, even rodlike polymeric molecules are known to fold or bend in solution. It is consistent, however, with the short relaxation times observed with NMR.[46] A careful analysis of the small q region at 40 °C shows that some longer cylindrical objects are present in the liquid phase ($\sim$1000 $\pm$ 50 Å long and $\sim$17 $\pm$ 4 Å in diameter). No changes take place in this regime with increasing temperature, and this indicates that this contribution arises from longer oligomers in the solution (the polydispersity of the polymer is 2).

With cooling below 40 °C, the line shape changes, as can be seen in the pattern measured at 30 °C. Although the solution still flows, this pattern cannot be fit with a cylindrical form factor. Further cooling leads to the formation of a phase, which macroscopically does not flow, exhibiting a neutron pattern similar to that at 30 °C. In the gel-like phase, the scattering intensity increases significantly, and the line shape changes. Although the system appears to be like a gel, the neutron patterns cannot be fit to a simple physical thermoreversible gel, in which single chains form a network. A network of large, flat aggregates has been considered on the basis of several different observations. These include NMR and enthalpy measurements, the viscous nature of the sample, the layered structure[45] reported in the solid state of PPE in the absence of a solvent in the bulk, and ribbonlike micrometer-length clusters observed with atomic force microscopy. A schematic representation of the phase diagram of the specific PPE under consideration is given in Figure 10.

For thin, flat aggregates, for which the length and width of the cluster are much larger than the thickness, the scattering function is given by $I(q)$

$= A(2\pi/q^2)(\Delta\rho)^2T^2\exp(-q^2R_t^2)$, where R_t is equal to $T/\sqrt{12}$ and T is the thickness of a flat particle.[33] Plotting $\ln(q^2I)$ as a function of q^2 [Fig. 9(b)] provides the thickness of the aggregate. At 40 °C, the line shape is that of a rigid rod and not that of a flat aggregate, as discussed before. With cooling to 30 °C, well-defined aggregates, with a thickness of approximately 46 Å, can be observed. The thickness can be evaluated within ±4 Å. At this temperature, NMR and DSC data show that some aggregation takes place, but the system is macroscopically fluid. Further cooling leads to the formation of the gel-like phase, which reveals aggregates of $T \sim 62$ Å, as shown at 25 °C. The thickness does not change as the temperature is further reduced.

The interactions between the PPE molecules and the solvent and the aggregation process have been further studied with various concentrations of the polymer. PPE is highly conjugated, and so attractive π–π interactions contribute to the interparticle interaction. This interaction is important to the interactions of the PPE molecules not only among themselves but with the solvent molecules as well. The structure of the PPE molecule in toluene has been followed at 40 °C as a function of the concentration between 0.11 and 4.08 wt %. At this temperature, all the solutions in this concentration range consist of isolated molecules. This concentration is well below the liquid crystallinity threshold of 15 wt % according to the Onsager theory.[56]

The density of the molecules in the molecular solution affects the flexibility of the PPE molecules. Shown in Figure 11(a) are SANS profiles at 40 °C at the indicated PPE concentrations. The scattering profiles of the 4.08 and 2.08 wt % solutions are consistent with a cylindrical form factor. The divergence of the scattering intensity at low q suggests that the individual, stretched PPE chains are still in contact with one another, forming loosely connected large networks.

The rodlike conformation of PPE molecules may be rationalized by their molecular density in solution. At these concentrations, the relatively close distance between individual PPE chains limits molecular rotation and translation in solution and, therefore, forces the stretched structure of the polymers. As the concentration of the PPE chains is reduced, the distance between isolated PPE chains increases. When the interpolymer chain distance becomes large enough, the confinement is reduced, and this allows the polymers to move more freely. In other words, the polymers become more flexible at lower concentrations, and this allows the bending of polymer chains.

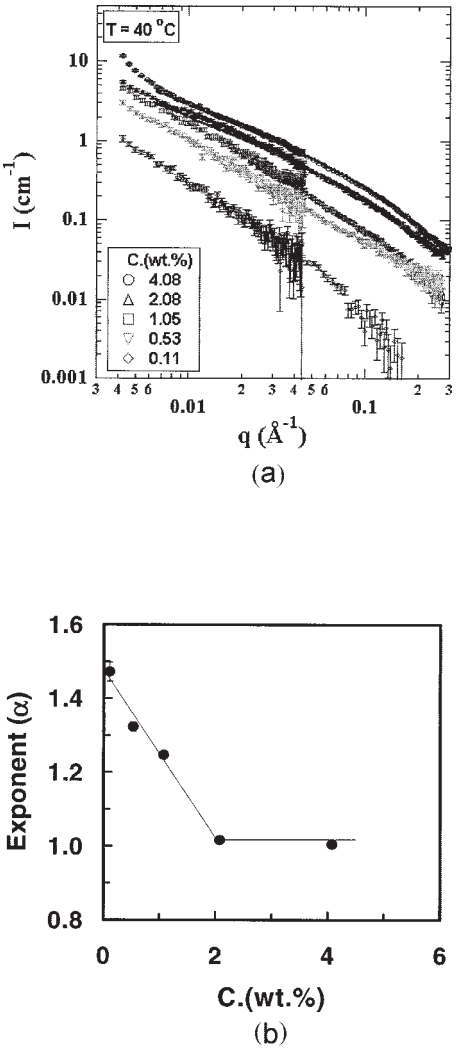

Figure 11. (a) SANS profiles at different concentrations of PPE at 40 °C. The symbols correspond to the experimental data. The solid lines are theoretical SANS profiles calculated for a cylindrical object with a radius of 10.5 Å and a length of 649 Å. (b) Plot of exponent α as a function of the concentration (C) fitted to $I(q) \propto q^{-\alpha}$.

When the concentration drops to 1.05 wt %, the profiles are not consistent anymore with a cylindrical form factor. The deviation of scattering profiles from a cylindrical form factor becomes larger when the concentration is further reduced. This can be demonstrated by a comparison of the slopes of the scattering profiles in a low q region, in which shape of the profiles is mainly governed by the conformation of the main chains. The slopes obtained by the fitting of about 1 decade of data points to a power law for different concen-

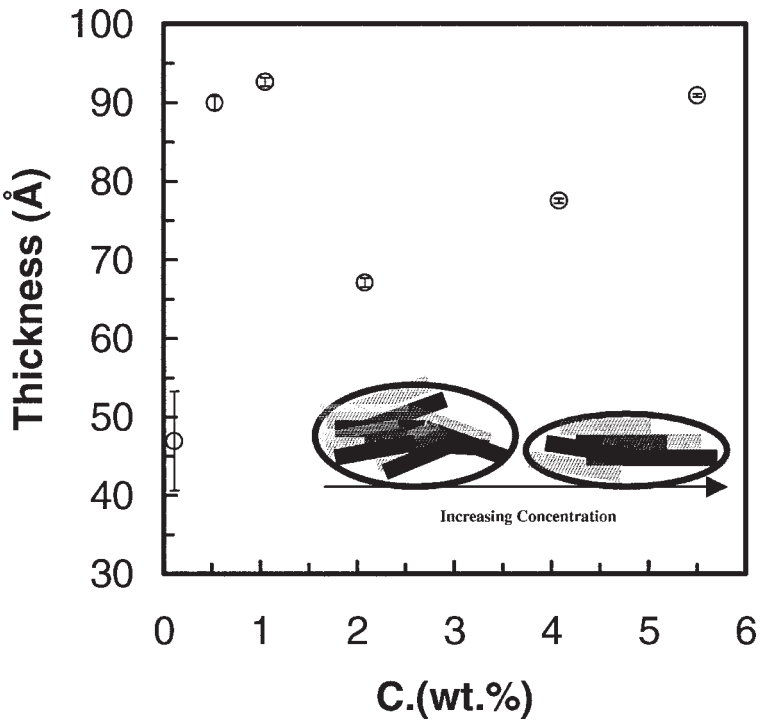

Figure 12. Thicknesses of the flat aggregates as extracted from the slopes of $\ln(q^2I)$ versus q^2. The insert shows a schematic model of the formation of an aggregate.

trations are shown in Figure 11(b). In dilute polymer solutions, the scattering intensity $I(q)$ scales with q as $I(q) \sim q^{-\alpha}$, where α is an effective exponent, and is specific to a particular polymer chain.[25,33] For a flexible Gaussian chain, $I(q)$ is approximately equal to q^{-2}; for a chain with excluded volume,[33] $I(q)$ is approximately equal to $q^{-1.66}$; and for rigid-rod polymers, $I(q)$ is approximately equal to q^{-1}. In other words, the scaling exponent increases as the chain flexibility increases.

As shown in Figure 11(b), the scaling exponent α increases with decreasing concentration. For 4.08 and 2.08 wt %, the slopes are close to 1, and this confirms the presence of rigid-rod polymers in solutions. The slope jumps to 1.28 when the concentration is reduced to 1.05 wt %. At the lowest concentration (0.11 wt %), the scaling exponent is 1.49, which is still lower than that of Gaussian chain and a chain with excluded volume. At these low concentrations, the coupling must occur via the solvent molecules. This is consistent with our previous NMR data,[46–47] which have shown that the relaxation time of toluene in the molecular solution differs from that of pure toluene. Previous studies[57] with light scattering have shown that much longer PPE polymers exhibit wormlike chains for which l_p is approximately 15 nm. The PPE polymer in this study is much shorter (~64 nm) and cannot be described as a wormlike chain.

As the solutions are cooled to 15 °C, all the solutions, with the exception of the 0.11 wt % solution, form a fragile gel phase. The thickness of the aggregates at this temperature is shown in Figure 12. With increasing concentration, the thickness increases up to 1.05 wt %, and then it drops. A further increase in the concentration results in a linear increase in the thickness. This trend is consistent in several independent experiments. The variation of the aggregate thickness can be rationalized in terms of a different density of packing of PPE molecules within the aggregates. At lower concentrations, the association of the PPE molecules is less dense and less ordered and so occupies more volume. With increasing concentration, a more ordered structure, similar to that observed in the bulk[45] and in thin films, is formed, initially occupying less volume. These structures then grow further. A tentative schematic representation of the formation of an aggregate is given as an insert in Figure 12. Because $\Delta\rho$ of an aggregate, in comparison with that of the solvent, depends on the number of solvent molecules associated with the cluster, an independent measure of either the size of the cluster or the

number of solvent molecules inside the aggregate is required to verify the model.

Conclusions

SANS measurements have shown that in molecular solutions, PPE is highly elongated. The interaction of PPE molecules with the solvent is rather high, affecting the conformation in molecular solutions and the density of PPE molecules within the aggregates. With increasing concentration or decreasing temperature, PPE molecules associate into flat aggregates. These grow and eventually jam into one another. NMR and neutron spin echo[58] studies have shown that this jamming together with the highly interacting solvent molecules results in a constraint of the motion of not only the aggregates but the solvent molecules as well.

CONCLUSIONS

With SANS, we have probed the molecular conformation of two highly interacting polydispersed polymers, a perfluorinated ionizable polymer and a rigid-rod polymer. The highly interactive mode, either by ionic interactions or by π–π couplings, results in extended polymer molecules in solution. When associated, the ionic polymer forms a highly charged, well-defined rodlike micelle, whereas the PPE molecules, governed by π–π stacking, form large, flat aggregates that jam into one another to form a fragile phase.

In both types of complex fluids formed by highly interacting polymers, well-defined aggregates are formed, although the chemical structure of the polymer is not well defined.

Tuning the chemical structure and following the effects of these chemical changes on the association mode will provide further insight into the association of these molecules. The dynamic behavior of both systems is currently under investigation with neutron spin echo, with the goal of correlating the molecular architecture with the structure and properties of highly interacting polymers.

The authors thank Boualem Hammouda, Steve Klien, and Charles Glinka from the Center for Neutron Research at the National Institute of Standards and Technology and Kenneth Littrell and Jyotsana Lal from the Intense Pulse Neutron Source of Argonne National Laboratory for fruitful discussions. They acknowledge Daryl D. DesMarteau from Clemson University for the synthesis of the perfluoroionomers and Uwe H.-F. Bunz from Georgia Tech for the synthesis of the poly(*p*-phenylene ethynylene) molecules. They kindly acknowledge the support of the National Science Foundation through the Center for Advanced Engineering Fibers and Films at Clemson University, the U.S. Department of Energy for the beam, the Educational Division of Argonne National Laboratory for the support of a student, and the Royal Thai Government for the support of R. Traiphol during this study.

REFERENCES AND NOTES

1. Bates, F. S.; Fredrickson, G. H. Phys Today 1999, 52(2), 32.
2. Matsen, M. W.; Bates, F. S. J Chem Phys 1997, 106, 2436.
3. Halperin, A.; Tirrell, M.; Lodge, T. P. Adv Polym Sci 1992, 100, 31–71.
4. Gottesfeld, S.; Zawodzinski, T. A. In Advances in Electrochemical Science and Engineering; Alkire, R. C.; Geridches, H.; Kdb, D. M.; Tobias, C. W., Eds.; Wiley-VCH: New York, 1997; Vol. 5, p 195.
5. Atkins, J. R.; Sides, C. R.; Creager, S. E.; Harris, J. L.; Pennington, W. T.; Thomas, B. H.; DesMarteau, D. D. J New Mater Electrochem Syst 2003, 6, 9–15.
6. Bronich, T. K.; Nehls, A.; Kabanov, V. A.; Eisenberg, A.; Kabanov, A. Polym Prepr (Am Chem Soc Div Polym Chem) 1998, 39, 2.
7. Guenet, J. M. J Phys Chem B 2002, 106, 2160.
8. Shetty, A. S.; Zhang, J.; Moore, J. S. J Am Chem Soc 1996, 118, 1019 and references therein.
9. Mio, M. J.; Prince, R. B.; Moore, J. S.; Kuebel, C.; Martin, D. C. J Am Chem Soc 2000, 122, 6134.
10. Deans, R.; Kim, J.; Machacek, M. R.; Swager, T. M. J Am Chem Soc 2000, 122, 8565.
11. Perahia, D.; Jiao, X.; Shmueli, L.; Gottlieb, M. J Chem Phys, in press.
12. Wignall, G. D.; Benoit, H.; Hashimoto, T.; Higgins, J. S.; King, S.; Lodge, T. P.; Mortensen, K.; Ryan, A. J. Macromol Symp 2002, 190, 185.
13. Melnichenko, Y. B.; Wignall, G. D.; Schwahn, D. Fluid Phase Equilib 2003, 212, 209.
14. Rathgeber, S.; Gast, A. P.; Hedrick, J. L. Appl Phys A 2002, 74(Suppl. 1), 396.
15. Kumar, S.; Naqvi, A. Z.; Aswal, V. K.; Goyal, P. S.; Kabir-ud-Din. Curr Sci 2003, 84, 1346.
16. Iatrou, H.; Hadjichristidis, N.; Meier, G.; Frielinghaus, H.; Monkenbusch, M. Macromolecules 2002, 35, 5426.
17. Chen, W.-R.; Chen, S.-H.; Mallamace, F. Phys Rev E: Stat Nonlinear Soft Matter Phys 2002, 66, 021403.
18. Galant, C.; Amiel, C.; Wintgens, V.; Sebille, B.; Auvray, L. Langmuir 2002, 18, 9687.
19. Mason, T. G.; Lin, M. Y. Phys Rev E: Stat Nonlinear Soft Matter Phys 2003, 67, 050401/1–050401/4.

20. Krishnamoorti, R.; Graessley, W. W.; Zirkel, A.; Richter, D.; Hadjichristidis, N.; Fetters, L. J.; Lohse, D. J. J Polym Sci Part B: Polym Phys 2002, 4, 1768.
21. Chen, Y. Y.; Lodge, T. P.; Bates, F. S. J Polym Sci Part B: Polym Phys 2002, 40, 466–477.
22. Tucker, R. T.; Han, C. C.; Dobrynin, A. V.; Weiss, R. A. Macromolecules 2003, 36, 4404.
23. Stenstam, A.; Montalvo, G.; Grillo, I.; Gradzielski, M. J Phys Chem B 2003, 107, 12331.
24. Hirai, M.; Iwase, H.; Hayakawa, T.; Koizumi, M.; Takahashi, H. Biophys J 2003, 85, 1600.
25. Guinier, A. Small-Angle Scattering of X-Rays; Wiley: New York, 1955.
26. Guinier, A. Anal Phys 1939, 12, 161.
27. King, M. S. In Modern Techniques for Polymer Characterisation; Pethrick, R. A.; Dawkins, J. V., Eds.; Wiley: New York, 1999.
28. Flory, P. J. Statistical Mechanics of Chain Molecules; Interscience: New York, 1969.
29. Higgins, J. S.; Benoit, H. C. Polymers and Neutron Scattering; Oxford University Press: New York, 1994.
30. DesMarteau, D. D. J Fluorine Chem 1995, 72, 203.
31. Bunz, U. H. F.; Enkelmann, V.; Kloppenburg, L.; Jones, D.; Shimizu, K. D.; Claridge, J. B.; zur Loye, H.-C.; Leiser, G. Chem Mater 1999, 11, 1416.
32. Marshal, A. R.; Bunz, U. H. F. Macromolecules 2001, 34, 4688.
33. Glatter, O.; Kratky, O. Small Angle X-Ray Scattering; Academic: New York, 1982.
34. Sharp; P.; Bloomfield, V. A. Biopolymers 1968, 6, 1201.
35. (a) Spiteri, M. N.; Boue, F.; Lapp, A.; Cotton, J. P. Phys Rev Lett 1996, 77, 5218; (b) Buholer, E.; Boue, F. Macromolecules 2003, 10, 1021.
36. Grot, W. G.; Chadds, F. European Patent 0066369, 1982.
37. Martin, C. R.; Rhoades, T. A.; Ferguson, J. A. Anal Chem 1982, 54, 1639.
38. Aldebert, P.; Dreyfus, B.; Gebel, G.; Nakamura, N.; Pineri, M.; Volino, F. J Phys Fr 1988, 49, 2101.
39. Aldebert, P.; Dreyfus, B.; Pineri, M. Macromolecules 1986, 19, 2651.
40. Gebel, G. Polymer 2000, 41, 5829.
41. Hill, T. A.; Carroll, D. L.; Czrew, R.; Martin, C. W.; Perahia, D. J Polym Sci Part B: Polym Phys 2002, 41, 149.
42. Serpico, J. M.; Ehrenberg, S. G.; Fontanella, J. J.; Jiao, X.; Perahia, D.; McGrady, K. A.; Sanders, E. H.; Kellogg, G. E.; Wnek, G. E. Macromolecules 2002, 35, 5916.
43. Flory, P. J. Principals of Polymer Chemistry; Cornell University Press: New York, 1953.
44. Jiao, X.; Perahia, D.; Thomas, B.; Tu, M.-H.; DesMarteau, D. D.; Lal, J. Macromolecules, submitted for publication.
45. Traiphol, R.; Bunz, U. H. F.; Perahia, D. Macromolecules 2001.
46. Perahia, D.; Traiphol, R.; Bunz, U. H. F. J Chem Phys 2002, 117, 1827.
47. Traiphol, R.; Perahia, D.; Bunz, U. H. F. Macromolecules, submitted for publication.
48. Witten, T. A. Rev Mod Phys 1999, 71, 6376.
49. Philipse, A. P.; Wierenga, A. M. Langmuir 1998, 14, 49.
50. Kumar, S. K.; Douglas, J. F. Phys Rev Lett 2001, 87, 188301.
51. Liu, A. J.; Nagel, S. R. Nature 1998, 396, 21.
52. O'Hern, C. S.; Langer, S. A.; Liu, A. J.; Nagel, S. R. Phys Rev Lett 2001, 86, 111.
53. Cates, M. E.; Wittmer, J. P.; Broichard, J.-P.; Clauding, P. Phys Rev Lett 1998, 81, 1841.
54. Kapnistos, M.; Vlasoopoulos, D.; Fytas, G.; Mortensen, K.; Fleischer, G.; Roovers, J. Phys Rev Lett 2000, 85, 4072.
55. (a) Mallamace, M.; Gambadauro, P.; Nicali, N.; Tartaglia, P.; Liao, C.; Chen, S.-H. Phys Rev Lett 2000, 84, 5431; (b) Chen, S.-H.; Liao, C.; Fratini, E.; Baglioni, P.; Mallamace, F. Colloids Surf A 2001, 183, 95.
56. Grosberg, A.; Khokhlov, A. Statistical Physics of Macromolecules; Nauke: Moscow, 1989; p 193.
57. Cotts, P. M.; Swagner, T. M.; Zhou, Q. Macromolecules 1996, 29, 7323.
58. Rosov, N.; Bunz, U. H. F.; Perahia, P. In preparation.